

Longitudinal Functional Models with Structured Penalties

Madan G. Kundu¹, Jaroslaw Harezlak¹ and Timothy W. Randolph²

¹*Department of Biostatistics
Indiana University Fairbanks School of Public Health
Indianapolis, USA*

²*Biostatistics and Biomathematics Program
Fred Hutchinson Cancer Research Center
Seattle, USA*

Abstract: This paper addresses estimation in a longitudinal regression model for association between a scalar outcome and a set of longitudinally-collected functional covariates or predictor curves. The framework consists of estimating a time-varying coefficient function that is modeled as a linear combination of time-invariant functions but having time-varying coefficients. The estimation procedure exploits the equivalence between penalized least squares estimation and a linear mixed model representation. The process is empirically evaluated with several simulations and it is applied to analyze the neurocognitive impairment of HIV patients and its association with longitudinally-collected magnetic resonance spectroscopy curves.

Key words and phrases: Functional data analysis, longitudinal data, mixed model, structured penalty, generalized singular value decomposition

1 Introduction

Technological advancements and increased availability of storage of large datasets have allowed for the collection of functional data as part of time-course or longitudinal studies. In the cross-sectional setting, there have been many proposed methods for estimating a regression function in a so-called functional linear model (fLM). This function is a functional (continuous) analogue of a vector of (discrete) regression coefficients; it connects the scalar response, y to a functional covariate, $w \equiv w(s)$. Although these models have recently been well studied, extensions to longitudinally-collected functions have not received much attention.

Only recently longitudinal penalized functional regression (LPFR) and longitudinal functional principal component regression (LFPCR) approaches have been proposed to extend the cross-sectional fLM to a longitudinal setting by incorporating subject-specific random intercepts (Goldsmith et al., 2012; Gertheiss et al., 2013). A basic assumption in both LPFR and LFPCR is that the regression function remains constant over time. Consequently, these methods are not suited for situations in which the association between a functional predictor and scalar response may evolve over time. Here we propose a technique that extends the analysis of functional linear models by relating a scalar outcome to a functional predictor—both observed longitudinally—and estimates a time-dependent regression function.

The method fits into a generalized ridge regression framework by imposing a scientifically-informed quadratic penalty term into the estimation process. The extension of this framework to the longitudinal setting has two major advantages: 1) the regression function is allowed to vary over time; and 2) external or a priori information about the structure of the regression function can be incorporated directly into the estimation process. We formulate the estimation procedure within a mixed-model framework making the method computationally efficient and easy to implement.

Ramsay and Dalzell (1991) introduced the term functional data analysis (FDA) in the statistical literature. The cross-sectional fLM with scalar response can be stated as follows (see e.g., Yao and Müller, 2010)

$$E(y|W) = \mu_y + \int_{\Omega} W(s)\gamma(s)ds$$

where μ_y is the mean of y , Ω denotes the domain of the predictor functions $W(s)$, $s \in \Omega$, and $\gamma(s)$ is a square integrable function that models the linear relationship between the functional predictor and scalar response. We will assume that $W(\cdot)$ denotes a mean-centered function ($E[W(s)] = 0$ for almost all $s \in \Omega$).

As there is no unique $\gamma(\cdot)$ that solves this equation some form of regularization, or constraint, is required. For example, a common approach is to impose smoothness on $\gamma(\cdot)$. One approach to this is to expand both the regression function $\gamma(\cdot)$ and predictor functions $W(\cdot)$ in terms of B-splines and then obtain the regularized estimate of $\gamma(\cdot)$ (Ramsay and Silverman, 1997). Another approach

is to express the regression function $\gamma(\cdot)$ in terms of the empirical orthonormal basis obtained by the eigenfunctions of the covariance of $W(\cdot)$ (i.e., a Karhunen-Loève (K-L) expansion (see e.g., Müller, 2005)). A third approach, known as penalized functional regression (PFR) (Goldsmith et al., 2011), combines the above two methods. In PFR, a spline basis is used to represent $\gamma(\cdot)$ and a subset of empirical eigenfunctions is used to represent each $W(\cdot)$. Another approach is to use a wavelet basis, instead of splines or eigenfunctions, to represent the predictor functions (Morris and Carroll, 2006).

Here we adopt an approach by Randolph *et al.* (2012) which does not begin by explicitly projecting onto a pre-specified basis of functions. Instead, prior information about functional structure is incorporated into the estimation process by way of a penalty operator, L . This approach of “partially empirical eigenvectors for regression” (PEER) exploits the fact that a penalized least-squares regression estimate mathematically arises as a series expansion in terms of a set of basis functions determined *jointly* by the covariance (empirical functional structure) and the penalty (imposed structure); see also the Appendix 7. This naturally extends ridge regression (non-structured penalty) and smoothing penalties such as a second-derivative penalty (presuming a smooth regression function). Here we extend the scope of the PEER approach to the longitudinal setting in a manner that allows the estimated regression function $\gamma \equiv \gamma(t, \cdot)$ to vary with time.

An important concern for any regularization method is identifiability of the estimate; i.e., the lack of uniqueness or, possibly, its instability. In FDA this arises from the lack of invertibility of the empirical covariance operator: a finite number of predictor curves means the dimension of the range of this operator is finite and so, as an operator on an infinite-dimensional domain, it has a non-trivial null space. The philosophy behind a penalty-operator approach is that estimation is constrained to the subspace spanned by functions that are jointly determined by W and L . A sufficient condition for uniqueness of this estimate is to assume $\text{Null}(W) \cap \text{Null}(L) = \{0\}$; see (Engl, Hanke and Neubauer, 2000) or (Bjorck, 1996). We assume this throughout.

The problem we address involves repeated observations from each of N subjects. For each subject, i , at each observation time, t , we collect data on a scalar response variable, y , and a (idealized) predictor function, $W(\cdot)$. We are interested

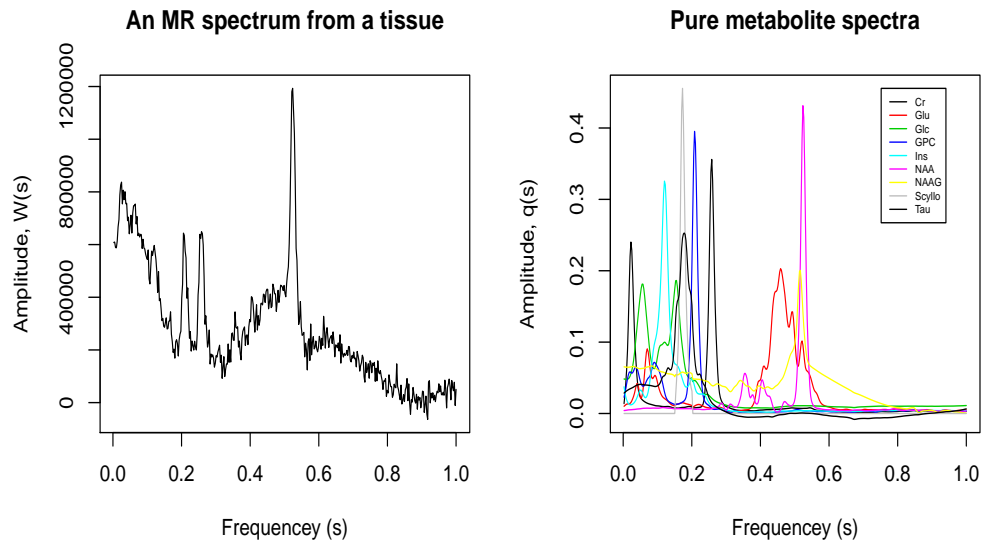


Figure 1: *Left panel:* an observed MR spectrum from tissue. *Right panel:* The 9 pure metabolite spectra. In each plot, the y -axis represents amplitude and x -axis the frequency of nucleus, s , transformed to $[0, 1]$ interval.

in longitudinal regression models of the form:

$$y_{it} = x_{it}^\top \beta + \int_0^1 W_{it}(s) \gamma(t, s) ds + z_{it}^\top b_i + \epsilon_{it}. \quad (1)$$

Here $\gamma(t, \cdot)$ denotes the regression function at time t , x_{it} is a vector of scalar-valued (non-functional) predictors; $z_{it}^\top b_i$ and ϵ_{it} denote the subject specific random effect and random error term, respectively. In a spirit similar to that of a linear mixed model with time-related slope for longitudinal data, we assume that $\gamma(t, \cdot)$ can be decomposed into several time-invariant component functions; e.g., $\gamma(t, \cdot) = \gamma_0(\cdot) + t \gamma_1(\cdot)$.

Our work is motivated by a study in which magnetic resonance (MR) spectra have been collected longitudinally from late stage HIV patients (Harezlak et al., 2011). We consider global deficit score (GDS) as a scalar response variable, y , and MR spectra as predictor functions, $W(\cdot)$. Of interest is the association of GDS with MR spectra and how this association evolves with time. One MR spectrum is shown in the left panel of Figure 1: the amplitude, $W(s)$, is plotted against the transformed frequency of nucleus, s , to the $[0, 1]$ interval (x -axis). The pattern and amplitudes of the peaks contain information about the concentration of metabolites present in tissue. Each metabolite has a *unique* spectrum and so one MR spectrum is a mixture of spectra from each individual metabolite (plus background and random noise); see the right panel in Figure 1 which displays spectra from 9 metabolites. Consequently, one expects an observed spectrum from tissue to lie near a functional subspace, \mathcal{Q} , spanned by the spectra of pure metabolites. The regression function, $\gamma(t, \cdot)$, models the association between y and $W(\cdot)$ and hence, in principle, should also lie near \mathcal{Q} . Hence, the subspace \mathcal{Q} should be more informative than B-splines or cosine functions that are in some sense “external” to the problem. For this reason, we adopt a methodology that encourages the estimate of $\gamma(\cdot)$ to be near to \mathcal{Q} . The approach is implemented using a *decomposition based penalty* which penalizes the estimate of $\gamma(t, \cdot)$ lightly if it belongs to \mathcal{Q} and strongly if it does not (Randolph *et al.*, 2012).

The cross-sectional fLM with scalar response has been a focus of various investigations (Ramsay and Silverman, 1997; Faraway, 1997; Fan and Zhang, 2000; Cardot, Ferraty and Sarda, 1999, 2003; Cai and Hall, 2006; Cardot et al., 2007; Reiss and Ogden, 2009), many of which estimate a regression function in

two steps. For example, Cardot, Ferraty and Sarda (2003) first perform principal component regression (PCR), which projects the observed predictor curves onto an empirical basis to obtain an estimate, then use B-splines to smooth the result. Reiss and Ogden (2009) study several of these methods along with modifications that include versions of PCR using B-splines and second-derivative penalties (cf. (Ramsay and Silverman, 1997; Silverman, 2009)). Extensions of fLM have been made towards generalized linear model with functional predictors (James, 2002; Müller and Stadtmüller, 2005) and quadratic functional regression (Yao and Müller, 2010). We are interested in extending the fLM to a longitudinal setting.

To our knowledge, the only published methods addressing the longitudinal functional predictor framework are LPFR (Goldsmith et al., 2012) and LFPCR (Gertheiss et al., 2013). The LPFR approach assumes the regression function in (1) is independent of time and proceeds in three steps: use a truncated set of K-L vectors to represent the predictor functions; express the regression function with a spline basis; fit the longitudinal model using an equivalent mixed-model framework that incorporates subject-specific random effects. In the LFPCR approach, the predictor functions are first decomposed into visit- and subject-specific functions accordingly via longitudinal functional principal component analysis (LF-PCA) (Greven et al., 2011) and in a second step, longitudinal analysis is carried out with the outcome of LFPCA. Both LPFR and LFPCR assume that the regression function, $\gamma(t, \cdot)$ remains constant over time. In contrast, we model the coefficient function $\gamma(t, \cdot)$ as a time-dependent linear combination of several time-invariant component functions, $\{\gamma_d(\cdot)\}_{d=0}^D$, each of which is estimated via a penalty operator that is informed by the structure of the data or a scientific question.

Section 2 establishes notation for the model considered in this paper. In Section 3.1, the concept of generalized ridge (Hoerl and Kennard, 1970) (or Tikhonov (1963)) estimation is discussed. We review a decomposition-based penalty in Section 3.2 and present how these estimates can be obtained as best linear unbiased predictors (BLUP) through mixed model equivalence in Section 4.1. Expressions for the precision of the estimates are derived in Section 4.2. In an Appendix (Section 7) we present how our longitudinal penalized estimate, along with its

bias and precision, can be obtained, under some weak assumptions, in terms of generalized singular vectors.

Numerical illustrations are provided by simulations in Section 5: Section 5.1 compares LPFR with the method proposed in this paper; Section 5.2 evaluates the influence of sample size and the effect of using prior functional information; Section 5.3 explores confidence band coverage probabilities; Section 5.4 evaluates performance when only partial information is available. An application to real MRS data using and a summary of our findings is presented in Section 5.5. The methods discussed in this paper have been implemented in the R package `refund` (Crainiceanu et al., 2012) via the `peer()` and `lpeer()` functions.

2 Statistical Model

We consider $\Omega = [0, 1]$, a closed interval in \mathbb{R} , and let $W(\cdot)$ denotes a random function in $L^2(\Omega)$. Let $W_{it}(\cdot)$ denotes a predictor function from the i^{th} subject ($i = 1, \dots, N$) at the t^{th} timepoint ($t = t_1, \dots, t_{n_i}$). Technically, an observed predictor arises as a discretized sampling from an idealized function, and we will assume that each observed predictor is sampled at the same p locations, $s_1, \dots, s_p \in [0, 1]$, with sampling that is appropriately regular and dense enough to capture informative functional structure, as seen, for instance, in the MRS data in Section 5.5. Let $w_{it} := [w_{it}(s_1), \dots, w_{it}(s_p)]^\top$ be the $p \times 1$ vector of values sampled from the realized function $W_{it}(\cdot)$. Then, the observed data are of the form $\{y_{it}; x_{it}; w_{it}\}$, where y_{it} is a scalar outcome, x_{it} is a $K \times 1$ column vector of measurements on K scalar predictors, and w_{it} is the sampled predictor from the i^{th} subject at time t . Denoting the true regression function at time t by $\gamma(t, \cdot)$, the longitudinal functional regression outcome model of interest is

$$y_{it} = x_{it}^\top \beta + \int_0^1 W_{it}(s) \gamma(t, s) ds + z_{it}^\top b_i + \epsilon_{it} \quad (2)$$

where, $\epsilon_{it} \sim N(0, \sigma_\epsilon^2)$ and b_i is the vector of r random effects pertaining to subject i and distributed as $N(0, \Sigma_{b_i})$. As usual we assume that z_{it} is a subset of x_{it} , ϵ_{it} and b_i are independent, ϵ_{it} and $\epsilon_{i't'}$ are independent whenever $i \neq i'$ or $t \neq t'$ or both, and b_i and $b_{i'}$ are independent if $i \neq i'$. Here $x_{it}^\top \beta$ is the standard fixed effect from K univariate predictors, $z_{it}^\top b_i$ is the standard random effect and

$\int_0^1 W_{it}(s)\gamma(t, s)ds$ is the subject/time specific functional effect. We assume that $\gamma(t, \cdot) \in L^2(\Omega)$, for all t .

The functional structure, indexed by s , and time structure, indexed by t , have somewhat unequal roles in our model, as we assume the longitudinal observations are more limited in the amount of information relative to the densely-sampled s index. For example, $\gamma(t, s)$ may vary linearly with time, $\gamma(t, s) = \gamma_0(s) + t\gamma_1(s)$, or quadratically, $\gamma(t, s) = \gamma_0(s) + t\gamma_1(s) + t^2\gamma_2(s)$. This is similar in spirit to a linear mixed effects model with linear or quadratic time slope (see e.g., Fitzmaurice, Laird and Ware, 2004). In general, we assume that $\gamma(t, s)$ can be decomposed into several time-invariant component functions $\gamma_0(s), \dots, \gamma_D(s)$ as

$$\gamma(t, s) = \gamma_0(s) + f_1(t)\gamma_1(s) + \dots + f_D(t)\gamma_D(s)$$

where, f_1, \dots, f_D are D prescribed linearly independent functions of t and $f_d(0) = 0$ for all d ; the time component t enters into $\gamma(t, s)$ through these terms. At $t = 0$, $\gamma(t, s)$ reduces to $\gamma_0(s)$ and has the obvious interpretation of a baseline regression function pertaining to the sampling points s . When $D = 0$, $\gamma(t, s) \equiv \gamma_0(s)$ is independent of t , a situation considered by Goldsmith et al. (2012). In general, each f may be any function of t with $f(0) = 0$, e.g., $f(t) = t$ or $t \exp(t)$. We can rewrite the equation (2) as

$$y_{it} = x_{it}^\top \beta + \int_0^1 W_{it}(s) \{ \gamma_0(s) + f_1(t)\gamma_1(s) + \dots + f_D(t)\gamma_D(s) \} ds + z_{it}^\top b_i + \epsilon_{it}$$

The association of y_{it} with W_{it} is modeled as a linear dependence on observations at p sampling points, w_{it} . In our approach, the (functional) structure is imposed directly into the estimation of each $\gamma_d = [\gamma_d(s_1), \dots, \gamma_d(s_p)]^\top$, for $d = 0, \dots, D$ (as described in Section 3). Combining all $n_\bullet = \sum_{i=1}^N n_i$ observations from the N subjects obtained across all time points, we express the model as

$$y = X\beta + W\gamma + Zb + \epsilon. \quad (3)$$

Here, $y = [y_{1t_1}, \dots, y_{1t_{n_1}}, \dots, y_{Nt_N}, \dots, y_{Nt_{n_N}}]^\top$ is a $n_\bullet \times 1$ vector of all responses, $X = [x_{1t_1}^\top, \dots, x_{1t_{n_1}}^\top, \dots, x_{Nt_N}^\top, \dots, x_{Nt_{n_N}}^\top]^\top$ is an $n_\bullet \times K$ design matrix pertaining to K univariate predictors, β is the associated coefficient vector, $\gamma = [\gamma_0^\top, \gamma_1^\top, \dots, \gamma_D^\top]^\top$ is a $(D+1)p \times 1$ vector of functional coefficients, W is the corresponding $n_\bullet \times (D+1)p$ design matrix. Further, b is the $n_\bullet \times 1$ vector of

random effects and Z is the corresponding $n_{\bullet} \times rN$ design matrix. The matrix W has the structure

$$W = \begin{bmatrix} W_1 \\ \vdots \\ W_N \end{bmatrix} \quad W_i = \begin{bmatrix} w_{it_1}^\top & f_1(t_1)w_{it_1}^\top & \cdots & f_D(t_1)w_{it_1}^\top \\ \vdots & \vdots & \ddots & \vdots \\ w_{it_{n_i}}^\top & f_1(t_{n_i})w_{it_{n_i}}^\top & \cdots & f_D(t_{n_i})w_{it_{n_i}}^\top \end{bmatrix}$$

3 Estimation of Parameters with a Penalty

Our approach builds on intuition from single-level functional regression that encourages an estimate of $\gamma(\cdot)$ to be in or near a “preferred” space via choice of penalty operator (Randolph *et al.*, 2012). To describe the effect of a general penalty operator, L , it is useful to consider the familiar example of a Laplacian penalty, \mathcal{L} . The typical heuristic for this arises by viewing β as a function whose local “smoothness” is informative. In this case, the term $\|\mathcal{L}\beta\|^2$ penalizes sharp changes in β . For our perspective, it is helpful to recall that the dominant eigenvectors of \mathcal{L} (those corresponding to the largest eigenvalues) are sharply oscillatory while the least-dominant eigenvectors are very smooth. Hence a linear-algebraic view of this is that rather than penalizing sharp changes, smoothness in the estimate is inherited from the eigenproperties of \mathcal{L} . More specifically, structure in the estimate arises from the joint eigenproperties of X and \mathcal{L} (as given by the GSVD). In general, the least-dominant eigenvectors of a penalty L will have the largest effect on the estimate. This property can be used to construct a “preferred subspace” by defining a penalty L whose least-dominant (or perhaps zero-associated) eigenvectors are preferred. The steps in PEER approach are as follows: (1) Identify the functional space where $W(\cdot)$ is expected to belong and treat this as a “preferred” space; (2) define a *decomposition-based penalty* (see Section 3.2) that penalizes more when the estimate of γ falls into the non-preferred space compared to preferred space. (3) Estimate $\gamma(\cdot)$ as a penalized estimate. In our longitudinal setting, we encourage the estimates for each of the $\gamma_0(\cdot), \dots, \gamma_D(\cdot)$ to be close to a preferred functional subspace. Our estimation approach allows the preferred subspace to be different for each of the $\gamma_d(\cdot)$ ’s. In the longitudinal (or t) dimension, γ is more explicitly and severely constrained by the choice of f_1, \dots, f_D .

3.1 Generalized Ridge Estimate

The model described in the previous section can be written as

$$y = X\beta + W\gamma + \epsilon^*, \quad (4)$$

where $\epsilon^* = Zb + \epsilon \sim N(0, V)$ and $V = Z\Sigma_b Z^\top + \sigma_\epsilon^2 I$. For each $d = 0, \dots, D$, let L_d be the penalty operator for γ_d and let λ_d^2 be the associated tuning parameter. The corresponding penalized estimates of β and γ are minimizers of:

$$\|y - X\beta - W\gamma\|_{V^{-1}}^2 + \lambda_0^2 \|\gamma_0\|_{L_0^\top L_0}^2 + \dots + \lambda_D^2 \|\gamma_D\|_{L_D^\top L_D}^2. \quad (5)$$

Here we use the notation $\|a\|_B^2 = a^\top B a$, where B is a symmetric, positive definite matrix. A generalized ridge estimate of β and γ based on minimizing the above expression is obtained as (see e.g., Ruppert, Wand and Carroll, 2003, p. 66)

$$\begin{bmatrix} \hat{\beta} \\ \hat{\gamma} \end{bmatrix} = (C^\top V^{-1} C + D)^{-1} C^\top V^{-1} y \quad (6)$$

where, $C = [X \ W]$, $D = \text{blockdiag}\{0, L^\top L\}$ and $L = \text{blockdiag}\{\lambda_0 L_0, \dots, \lambda_D L_D\}$.

In the Appendix, we derive an expression for the generalized ridge estimate $\hat{\gamma}$ explicitly in terms of the generalized singular value decomposition (GSVD) components.

3.2 Decomposition based penalty

Let $\gamma_d \equiv \gamma_{L_d, \lambda_d}$ be the estimate obtained from the penalty operator L_d and tuning parameter λ_d^2 , for each $d = 0, \dots, D$. For example, L_d may denote I_p (a ridge penalty) or a second-order derivative penalty (giving an estimate having continuous second derivative). Alternatively, with prior knowledge about potentially relevant structure in a regression function, a targeted decomposition-based penalty can be defined in terms of a subspace defined by such structure (Randolph *et al.*, 2012). To be precise, if it is appropriate to impose scientifically-informed constraints on the ‘‘signal’’ being estimated by γ , this prior may be implemented by encouraging the estimate to be in or near a subspace, $\mathcal{Q} \subset L^2(\Omega)$.

Returning to our notation that reflects functional predictors observed at p sampling points, we represent \mathcal{Q} by the range of a $p \times J$ matrix Q whose columns are q_1, \dots, q_J . Consider the orthogonal projection $P_Q = QQ^+$ onto

the $\text{Range}(Q)$, where Q^+ is Moore-Penrose inverse of Q . Then a decomposition penalty is defined as

$$L_Q = \phi_b P_Q + \phi_a (I - P_Q) \quad (7)$$

for scalars ϕ_a and ϕ_b . To see how L_Q works, let $\tilde{\gamma}_d$ be any estimate of γ_d . When $\tilde{\gamma}_d \in \text{span}(Q)$, we have $L_Q \tilde{\gamma}_d = \phi_b \tilde{\gamma}_d$, but when $\tilde{\gamma}_d \notin \text{span}(Q)$, we have $L_Q \tilde{\gamma}_d = \phi_a \tilde{\gamma}_d$. The condition $\phi_a > \phi_b$ imposes more penalty for $\tilde{\gamma}_d \notin \text{span}(Q)$ compared to when $\tilde{\gamma}_d \in \text{span}(Q)$. The weights ϕ_a and ϕ_b determine the relative strength of emphasizing Q in the estimation process. Note, in particular, that taking $\phi_a = \phi_b$ results in a ridge estimate and that L_Q is invertible, provided ϕ_a and ϕ_b are nonzero. Some analytical properties for this family of penalized estimates are discussed in Randolph *et al.* (2012).

4 Mixed model representation

Estimates of β and γ obtained by minimizing the expression in equation (5) correspond to a generalized ridge estimate. In this section we aim to construct an appropriate mixed model that minimizes the expression in equation (5). In general, the penalty, L , is not required to be invertible but for simplicity this will be assumed here. The mixed model approach provides an automatic selection of tuning parameters $\lambda_1, \dots, \lambda_D$. REML-based estimation of the tuning parameters has been shown to perform as well as the other criteria and under certain conditions it is less variable than GCV-based estimation (Reiss and Ogden, 2009).

4.1 Estimation of parameters

Using Henderson's justification (Henderson, 1950), one can show that, for each $d = 0, \dots, D$, the model $y = X\beta + W\gamma + \epsilon^*$ where, $\epsilon^* \sim N(0, V)$ and $\gamma_d \sim N(0, \frac{1}{\lambda_d^2} (L_d^\top L_d)^{-1})$, minimizes the expression in equation (5) to obtain the BLUP. Thus the generalized ridge estimate of β and γ correspond to the BLUP from the following model:

$$y = X\beta + W^*\gamma^* + \epsilon$$

where, $W^* = [W \ Z]$, $\gamma^* = [\gamma^\top \ b^\top]^\top \sim N[0, \Sigma_{\gamma^*}]$ and $\epsilon \sim N(0, \sigma_\epsilon^2 I)$ with

$$\Sigma_{\gamma^*} = \text{blockdiag}\{(L^\top L)^{-1}, \Sigma_b\} \quad \text{and} \quad \Sigma_b = \text{blockdiag}\{\Sigma_{b_1}, \dots, \Sigma_{b_N}\}.$$

This representation allows us to estimate fixed and functional predictors simply by fitting a linear mixed model (e.g., using the `lme()` of the `nlme` package in R or PROC MIXED in SAS).

4.2 Precision of Estimates

Our ridge estimate is the BLUP from an equivalent mixed model, hence the variance of the estimate depends on whether the parameters are random or fixed. Randomness of γ is a device used to obtain the ridge estimate while ϵ and b in our case are truly random. With this in mind, we follow Ruppert, Wand and Carroll (2003) and assume that the variance of the estimates is conditional on γ , but not on b . The BLUP of β , γ and b can be expressed as (see e.g., Robinson, 1991; Ruppert, Wand and Carroll, 2003):

$$\begin{aligned}\tilde{\beta} &= \left(X^\top V_1^{-1} X\right)^{-1} X^\top V_1^{-1} y & \tilde{\gamma} &= (L^\top L)^{-1} W^\top V_1^{-1} (y - X\tilde{\beta}) \\ \tilde{b} &= \Sigma_b Z^\top V_1^{-1} (y - X\tilde{\beta})\end{aligned}$$

where $V_1 = V + W(L^\top L)^{-1}W^\top$. $\tilde{\beta}$ is an unbiased estimator of β , but $\tilde{\gamma}$ is not unbiased. It is trivial to see that $\text{Cov}(y|\gamma) = V$. Thus, the variances of $\tilde{\beta}$ and $\tilde{\gamma}$, conditional on γ , are:

$$\begin{aligned}\text{Cov}(\tilde{\beta}|\gamma) &= \left(X^\top V_1^{-1} X\right)^{-1} X^\top V_1^{-1} V V_1^{-1} X \left(X^\top V_1^{-1} X\right)^{-1} \\ \text{Cov}(\tilde{\gamma}|\gamma) &= A_\gamma V A_\gamma^\top \quad A_\gamma = (L^\top L)^{-1} W^\top V_1^{-1} \{V_1 - X(X^\top V_1^{-1} X)^\top\} V_1^{-1}\end{aligned}\quad (8)$$

To obtain the unconditional variance, one must replace V by V_1 in the above expressions, but this will overestimate the variance of the estimates. Expressions for the predicted value of y and its variance are:

$$\tilde{y} = X\tilde{\beta} + W\tilde{\gamma} + Z\tilde{b} \quad \text{Cov}(\tilde{y}|\gamma) = A_y V A_y^\top$$

where $A_y = \{[V_1 - WL^\top LW - Z\Sigma_b Z^\top]^{-1} X (X^\top V^{-1} X)^{-1} X^\top V^{-1} + WL^\top LW^\top + Z\Sigma_b Z^\top\} V_1^{-1}$.

Let, $T = [1 \ f_1(t) \ \cdots \ f_d(t)] \otimes I_K$. Then the discretized version of regression function at time t is $\gamma_{(t)} = [\gamma(t, s_1), \dots, \gamma(t, s_K)] = T\gamma$. Therefore, the estimate of $\gamma_{(t)}$ is $\tilde{\gamma}_{(t)} = T\tilde{\gamma}$ and the estimate of its variance is $T\text{Cov}(\tilde{\gamma}|\gamma)T^\top$. The smoothing parameters' estimates are the ratios of the variance components in

the mixed model equivalence of the LongPEER model. The derivations above do assume the knowledge of the variance components' true values. In practice, these variance components are estimated and the empirical versions of the regression parameters are obtained (EBLUPs).

4.3 Selection of time-structure in $\gamma(t, \cdot)$

The proposed approach allows a flexible choice of the time structure to be included in the regression function $\gamma(t, \cdot)$. In practice, data and information to estimate structure of the longitudinal observations (along the t index) are more limited than the functional relationship along the s index. For example, whether $\gamma_0(t, \cdot) + t\gamma_1(t, \cdot)$ is sufficient or the more flexible $\gamma_0(t, \cdot) + t\gamma_1(t, \cdot) + t^2\gamma_2(t, \cdot)$ is required is not known. The problem of choosing appropriate time-structure in $\gamma(t, \cdot)$ is similar, in principle, to that of choosing time structure in a linear mixed-effects model (e.g., $E(y_{it}|b_i) = \beta_0 + \beta_1 t$ or $E(y_{it}|b_i) = \beta_0 + \beta_1 t + \beta_2 t^2$). We propose two approaches to decide what the form of unknown regression function is: (a) Use of the AIC to compare different structures, and (b) Use of the point-wise confidence band for the component functions: $\gamma_0(s), \dots, \gamma_D(s)$. If the confidence band for any $\gamma_d(s)$ contains zero in its entire domain, then such term is dropped from the $\gamma(t, s)$.

4.4 Selection of ϕ_a and ϕ_b for a decomposition penalty

We view ϕ_a and ϕ_b as weights of a tradeoff between preferred and non-preferred subspaces and assume $\phi_a \cdot \phi_b = \text{constant}$. In the current implementation, we use REML to estimate λ_d 's for a fixed value of ϕ_a , and do a grid search over the ϕ_a values to jointly select the tuning parameters which maximize the information criterion, such as AIC, based on the restricted maximum likelihood.

5 Simulation

We pursue several simulations to evaluate the properties of the LongPEER method. The first simulation study (Section 5.1) compares the performance of the LongPEER method with the LPFR approach. In the remaining simulation studies, only the LongPEER method is considered. The purpose of the second

simulation study is to evaluate the influence of sample size and the contribution of prior information about the functional structure (as determined by the tuning parameters ϕ_a and ϕ_b in (7)) on the LongPEER estimate. In the third simulation study, we evaluate the coverage probabilities of the confidence bands constructed using the formula presented in Section 4.2. Finally, we evaluate the performance of LongPEER estimate when information on some features is missing and the results are summarized in Section 5.4. In all the simulation studies, the simulated predictor functions resemble the MRS data. All results summarized in this Section are based on 100 simulated datasets.

For each subject and visit, predictor functions were simulated independently. Predictor functions were flat with bumps of varied widths at a number of pre-specified locations. White noise was added to the predictor functions to account for the instrumental measurement noise. These “bumpy” regression functions were generated with bumps at some (but, not all) of the bump locations of the predictor function. For the simulation in Section 5.1, the regression function is assumed to be independent of time, whereas it varies with time in the simulation of Section 5.2. For both the predictor and regression functions, 100 equi-spaced sampling points in $[0,1]$ are used.

For the decomposition penalty (7), the matrix L_d is defined as follows: 1) select the discretized functions $q_j, j = 1, \dots, J$ spanning the “preferred” subspace and 2) compute $L_d = QQ^+$, where $Q = \text{col}[q_1, \dots, q_J]$ and the vectors q_j are discretized functions, defined to have a single bump corresponding to a region in the simulated predictor functions; see Figure 2. The columns of Q need not be orthogonal (cf., Figure 9).

Estimation error is summarized in terms of the mean squared error (MSE) of the estimated regression function defined as $\|\gamma - \tilde{\gamma}\|^2$, where $\tilde{\gamma}$ denotes the estimate of γ . Further, MSE was decomposed into the trace of the variance and squared norm of bias. We also calculated the sum of squares of prediction error (SSPE) as $\|y - \tilde{y}\|^2/N$, where \tilde{y} denotes the estimate of the true (noiseless) y . The estimates based on the proposed methods, including the LongPEER estimate, were obtained as BLUPs from the mixed model formulation described in Section 4.1.

5.1 Comparison with LPFR

As mentioned, LPFR estimates a regression function that does not vary with time. Therefore, in the first set of simulations we generated outcomes using a time-invariant regression function (i.e., $\gamma(t, s) = \gamma_0(s)$, for all t). The following model was used to generate the outcome data for 100 individuals ($i = 1, \dots, 100$), each at 4 timepoints ($t = 0, 1, 2, 3$):

$$y_{it} = \beta_0 + \int_0^1 W_{it}(s)\gamma_0(s)ds + b_i + \epsilon_{it}, \quad i = 1, \dots, 100, \quad (9)$$

$$\text{where,} \quad \gamma_0(s) = \sum_{h \in H_{\gamma_0}} a_{0h} \exp \left[-2500 * \left(\frac{h-s}{100} \right)^2 \right].$$

The bumpy predictor functions were generated from the following equation

$$\begin{aligned} w_{it}(s) = & \sum_{h \in H_1} (\xi_{1h} + c_{1h}) \exp \left[-2500 * \left(\frac{s-h}{100} \right)^2 \right] \\ & + \sum_{h \in H_2} (\xi_{2h} + c_{2h}) \exp \left[-1000 * \left(\frac{s-h}{100} \right)^2 \right] \\ & + (\xi_{31} + 0.9) \exp \left[-250 * \left(\frac{s-50}{100} \right)^2 \right], \end{aligned} \quad (10)$$

where c_{1h} , c_{2h} and a_{0h} are defined in Table 1. $\{\xi_{1h}, h \in H_1\}$, $\{\xi_{2h}, h \in H_2\}$, and ξ_{31} were drawn independently from Uniform(0, 0.1). Also, $\beta_0 = 0.06$, $\epsilon_{it} \sim N[0, (0.02)^2]$ and $b_i \sim N[0, (0.05)^2]$.

Table 1: Values of c_{1h} , c_{2h} , a_{0h} and a_{1h} for generating predictor and regression function in simulation studies in Sections 5.1, 5.2, 5.3 and 5.4.

$h \in H_1$		$h \in H_2$		$h \in H_{\gamma_0}$		$h \in H_{\gamma_1}$	
h	c_{1h}	h	c_{2h}	h	a_{0h}	h	a_{1h}
15	0.10	30	0.60	15	0.20	30	0.06
5	0.10	70	0.50	50	-0.15	70	-0.06
		80	0.50	80	0.15		
		90	0.40				

We applied both LPFR (using `lpfr()` available in the `refund` package in R (Crainiceanu et al., 2012)) and the LongPEER method to the simulated data.

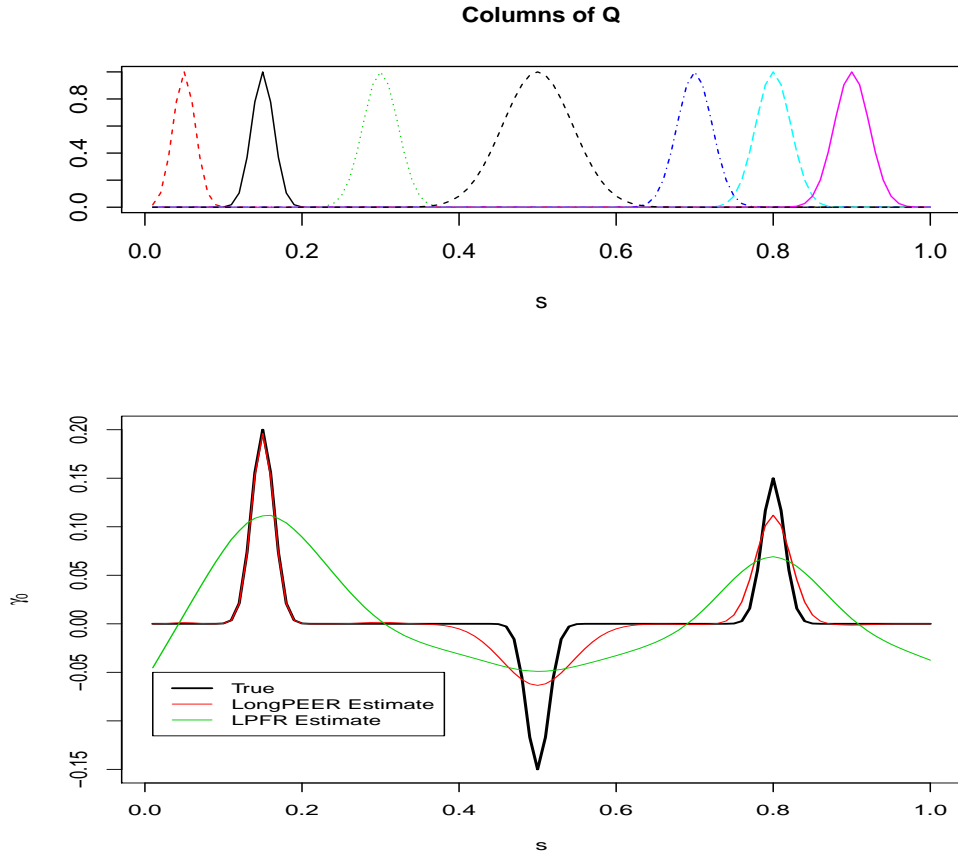


Figure 2: Average estimates of γ for the simulation in Section 5.1 with $\phi_a = 10$ and $\phi_b = 1$. *Top panel:* columns of Q used in the decomposition penalty. *Bottom panels:* the true γ and the average of estimates from 100 simulations.

Table 2: Estimation and prediction errors for LPFR and LongPEER estimates based on 100 simulated datasets. The sample size is $N = 100$ and the number of longitudinal observations is $n_i = 4$.

	LongPEER	LPFR
MSE(γ_0)	0.0323	0.2244
Trace of Variance(γ_0)	0.0028	0.0490
$\ \text{Bias}(\gamma_0)\ ^2$	0.0295	0.1754
SSPE of Y	1.1566	1.1535

To obtain the LPFR estimate, the dimension of both principal components for predictor function and truncated power series spline basis for the regression function were set to 60. The columns of Q used to define L_Q , for the LongPEER estimate are plotted in the top panel of Figure 2. We used $\phi_a/\phi_b = 10$, a choice motivated by our findings in Sections 5.2 and 5.4.

Table 2 displays the MSE and prediction error obtained for LongPEER and LPFR estimates. The SSPE was similar for both methods (1.1566 and 1.1535), however, the LongPEER estimate has smaller MSE. Both the bias and variance are higher for the LPFR estimate and consequently it has the greater MSE. Figure 2 displays the estimates of the regression function. It should be emphasized that any comparison of these methods is not entirely fair since LongPEER is designed to exploit presumed structural information while LPFR is not. We note also that the ability to exploit such information may be limited and so in this simulation we used imprecise information about the shapes of features; see top panel in Figure 2. Not surprisingly, performance is best for the feature at $s = 0.15$ where information about the shape was relatively precise. See also Section 5.4.

5.2 Simulation with a time varying regression function

Here the regression function varies parametrically with time. Lacking other functional regression methods that estimate a time-varying regression function, we only evaluated the performance of LongPEER. The primary goal was to assess the effects of sample size, fraction of variance explained by the model, and the relative contribution of external information (as determined by ϕ_a and ϕ_b in equation 7) on estimate.

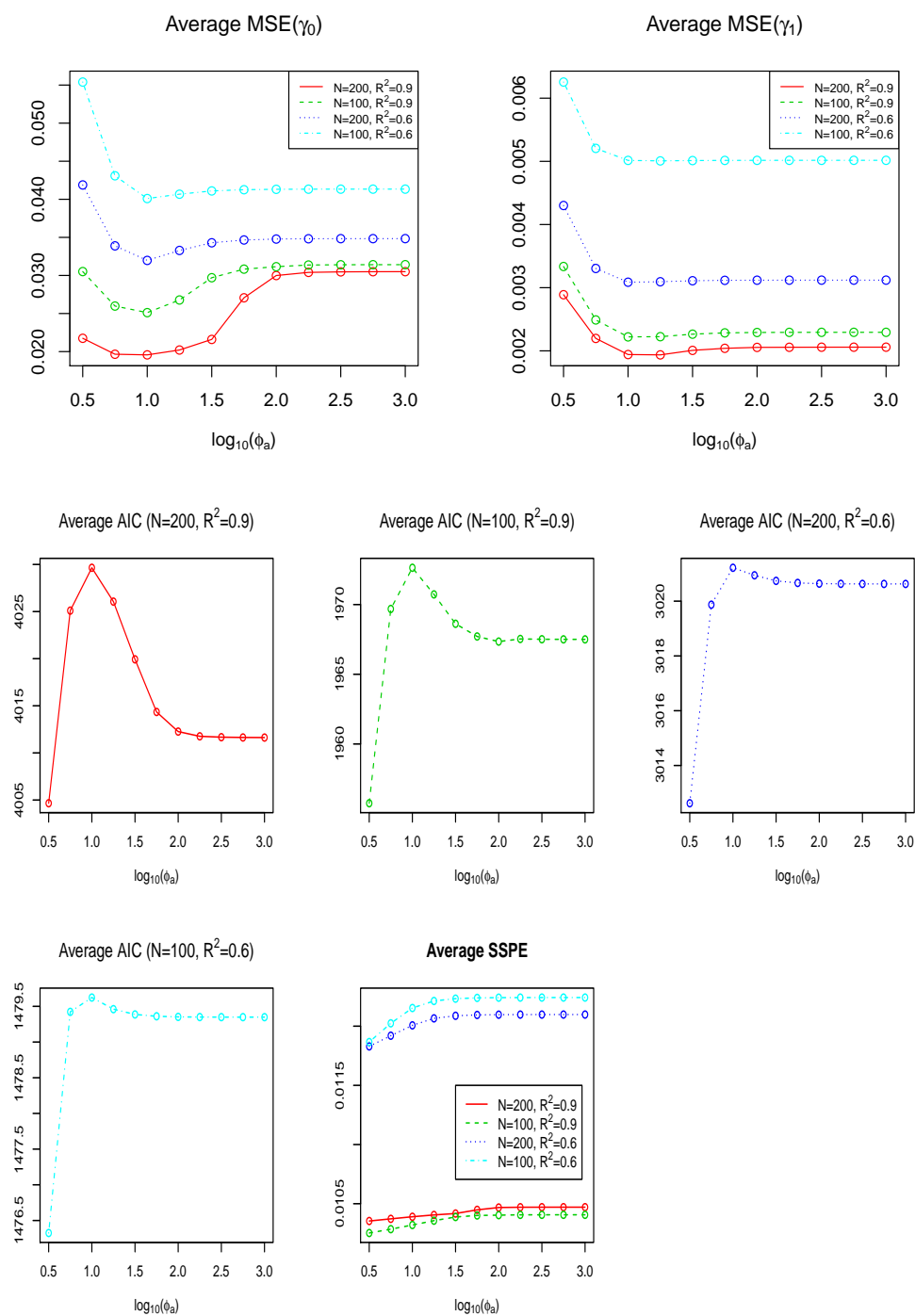


Figure 3: Average AIC, SSPE and MSE for simulations in Section 5.2 over 100 simulations. At $\phi_a = 10$, average AIC were maximized and $\text{MSE}(\gamma_0)$ and $\text{MSE}(\gamma_1)$ were minimized. In general, average AIC increased with the increase in sample size and R^2 whereas SSPE, $\text{MSE}(\gamma_0)$ and $\text{MSE}(\gamma_1)$ decreased.

Without loss of generality, we set $\phi_b = 1$ and vary ϕ_a on an exponential scale. Larger values of ϕ_a indicate greater emphasis of prior information on the estimation process. The model considered here is similar to that described in Section 5.1 with the exception that $\gamma(t, s) = \gamma_0(s) + t \gamma_1(s)$. The function $\gamma_0(s)$ is defined in equation (10) and $\gamma_1(s)$ is of the form

$$\gamma_1(s) = \sum_{h \in H_{\gamma_1}} a_{1h} \exp \left[-2500 * \left(\frac{h-s}{100} \right)^2 \right]$$

where the value of h and a_{1h} are listed in Table 1 and $\beta_0 = 0.06$. Realizations of functional predictors were generated as described in section 5.1. For each simulation, an appropriate σ_ϵ^2 was chosen to ensure that the squared multiple correlation coefficient $R^2 = s_y^2 / [s_y^2 + \sigma_\epsilon^2]$ is 0.6 and 0.9. Here, $s_y^2 = \frac{1}{4} \sum_{t=0}^3 \frac{1}{N-1} \sum_{i=1}^N (y_{it} - \bar{y}_{.t})^2$ denotes the average sample variance in the set $\{y_{it} - \epsilon_{it} : i = 1, \dots, N; t = 0, \dots, 3\}$ with $\bar{y}_{.t} = \frac{1}{N} \sum_{i=1}^N y_{it}$.

We have repeated the simulation for four scenarios: (i) $N = 100$, $R^2 = 0.6$; (ii) $N = 100$, $R^2 = 0.9$; (iii) $N = 200$, $R^2 = 0.6$; and (iv) $N = 200$, $R^2 = 0.9$. Estimate of γ_0 and γ_1 were obtained using a decomposition penalty. The columns of Q used to define L_Q are plotted in the top panel of Figure 5. Results for AIC, MSE and SSPE are displayed graphically in Figure 3. The standard deviation of MSE were plotted in Figure 4. As the sample size and R^2 increased, both the $\text{MSE}(\gamma_0)$ and $\text{MSE}(\gamma_1)$ were decreased, providing empirical evidence that the LongPEER estimates were consistent. In all four scenarios, $\text{MSE}(\gamma_0)$ was minimized at $\phi_a = 10$, it increased with ϕ_a up to $\phi_a = 100$, and plateaued after that. On the other hand, a decrease in $\text{MSE}(\gamma_1)$ is observed as ϕ_a increased up to 10 and it plateaued thereafter. That is, an increase in ϕ_a up to 10 resulted in improvement in estimation of both γ_0 and γ_1 . However, ϕ_a beyond 10 resulted in deterioration in performance of estimation for γ_0 ; estimation performance for γ_1 remained almost unchanged. To understand this result, we need to compare the plots of columns for Q matrix used in defining L_Q with true γ_0 and γ_1 in Figure 5: γ_0 has peaks at $s = 0.2, 0.5$ and 0.8 . and Q contains functions (columns) representing peaks at these locations. However, the shape of the peak at $s = 0.5$ is different from that in γ_0 . Due to this difference in shape, as ϕ_a increased from 10 to 100, the feature at $s = 0.5$ in $\tilde{\gamma}_0$ became smaller leading to gradual increase in $\text{MSE}(\gamma_0)$. On the other hand, γ_1 has two features while Q contains

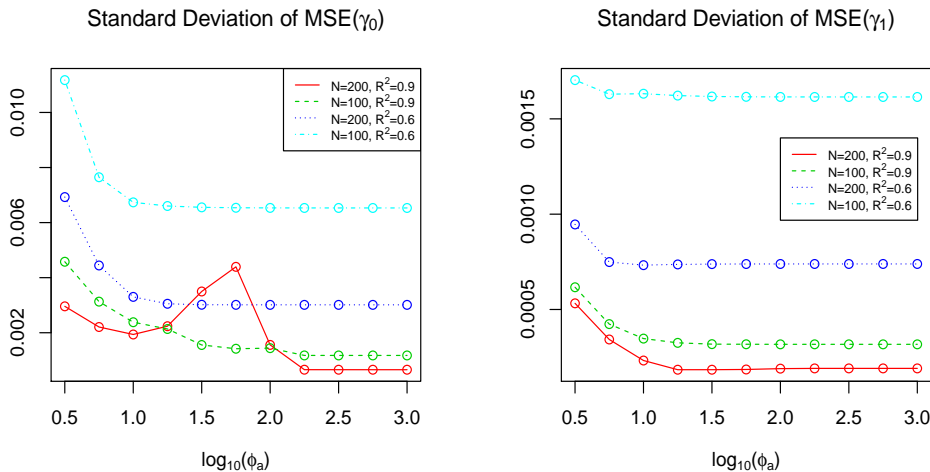


Figure 4: Standard deviation of MSE for simulations in Section 5.2 over 100 simulations. Standard deviation of $\text{MSE}(\gamma_0)$ and $\text{MSE}(\gamma_1)$ generally decrease with increasing sample size and R^2 . $\text{MSE}(\gamma_0)$ and $\text{MSE}(\gamma_1)$ both decrease up to $10^{1.25}$ and then plateau, except for $\text{MSE}(\gamma_0)$ in the scenario with $N = 200$ and $R^2 = 0.9$.

functions of very similar shape. Consequently, $\text{MSE}(\gamma_1)$ stabilizes after $\phi_a = 10$. Finally, note that the value of ϕ_a that maximized AIC also minimized $\text{MSE}(\gamma_0)$ and $\text{MSE}(\gamma_1)$. This suggests that AIC can be used to guide the choice of ϕ_a while setting ϕ_b at 1. In general, the choice of ϕ_a may be take as that which maximizes AIC.

The average LongPEER estimate of γ_0 and γ_1 using a decomposition penalty are displayed in Figure 5 with $\phi_a = 10$ and $\phi_b = 1$. For smaller sample sizes and R^2 , the LongPEER estimate may: (a) oversmooth (i.e., negatively bias) the estimated regression function at locations of a true feature, and (b) be positively biased in locations corresponding to features in \mathcal{Q} but where the true γ is zero. However, by increasing the sample size to 200 and/or R^2 to 0.9, we observe that the average LongPEER estimate $\gamma_0(\cdot)$ and $\gamma_1(\cdot)$ approach the true functions.

5.3 Coverage probability

In this section, we used the simulation setup described in Section 5.2 with $R^2 = 0.9$. The columns of Q matrix used in defining the decomposition penalty (7)

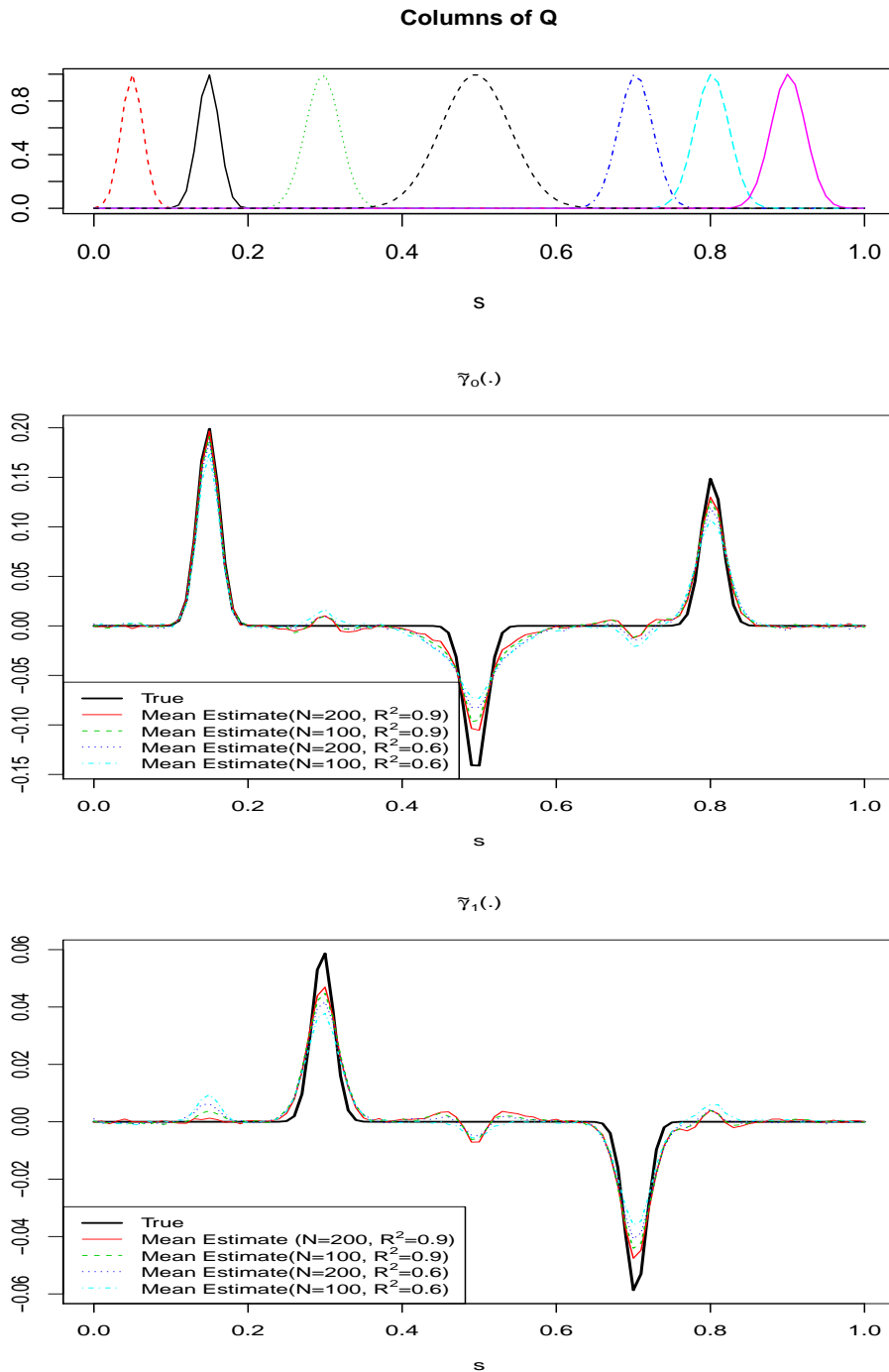


Figure 5: Average estimates of the components of regression functions for simulations described in Section 5.2 with $\phi_a = 10$ and $\phi_b = 1$. *Top panel:* columns of Q used in defining a *decomposition penalty*. *Middle and bottom panels:* the average estimates of γ_0 and γ_1 ; these improve as N and/or R^2 increase.

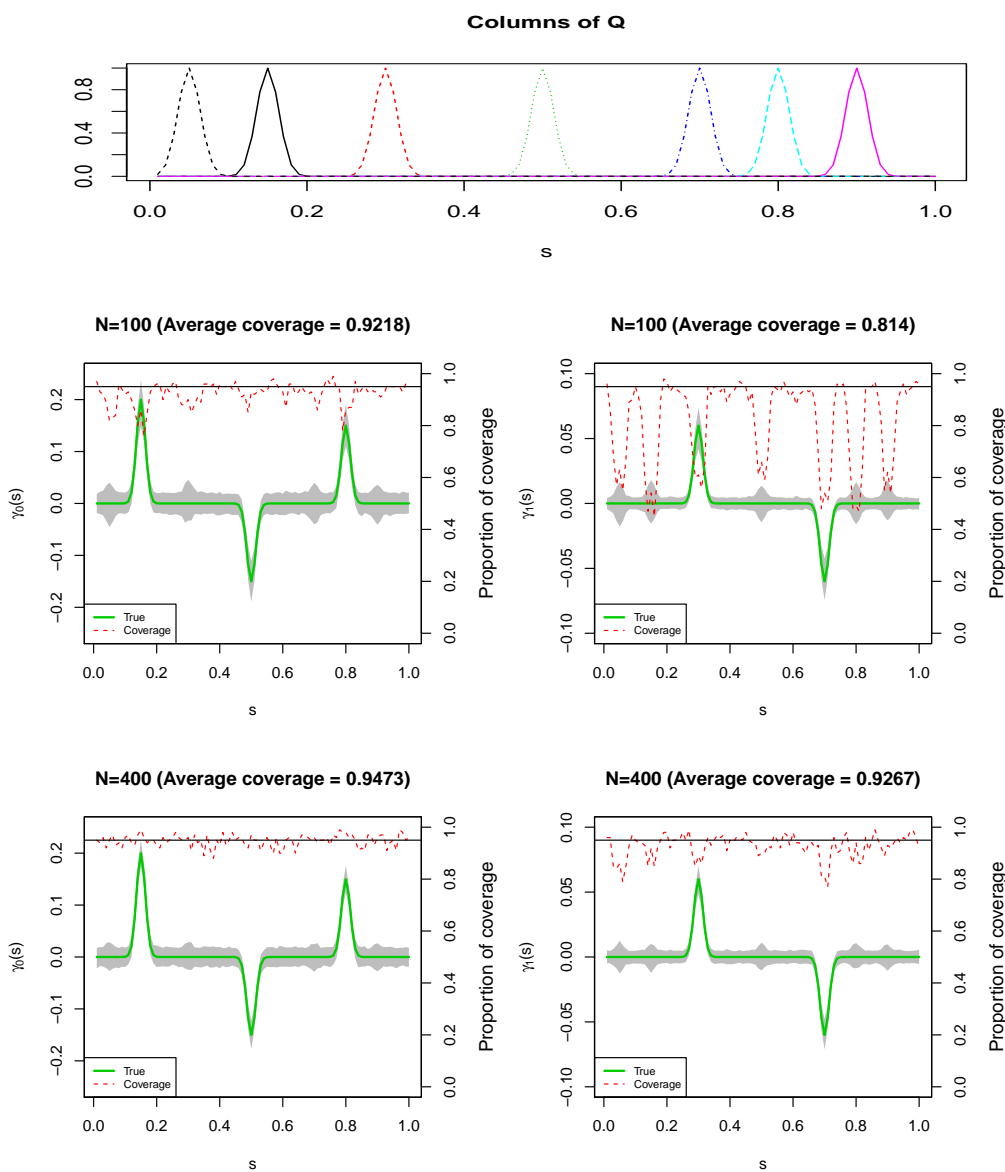


Figure 6: Coverage probabilities of LongPEER estimates in 100 simulations with $\phi_a = 10$ and $\phi_b = 1$ discussed in section 5.3. *Top panel:* the columns of Q used in the *decomposition penalty*. *Middle and bottom panels:* pointwise 95% confidence band (shaded region) and coverage proportions (the dotted line) based on $N = 100$, and $N = 400$ subjects, respectively. The left column displays the cross-sectional function $\gamma_0(\cdot)$ and the right column the longitudinal function $\gamma_1(\cdot)$. The horizontal line in each plot marks the nominal coverage of 95%.

are displayed in the top panel of Figure 6. The middle and bottom panel shows the confidence bands and the coverage probabilities obtained using $\phi_a = 10$. The 95% confidence bands are constructed as $Estimate \pm 1.96 \times (Standard\ Error)$. When the sample size N increased, there was a notable improvement in coverage of both $\gamma_0(\cdot)$ and $\gamma_1(\cdot)$. For $N = 100$, the coverage of $\gamma_1(\cdot)$ by the confidence bands was only around 81%. This confidence band under-coverage of $\gamma_1(\cdot)$ is caused by the comparatively larger bias in the estimation of $\gamma_1(\cdot)$ with $N = 100$ (see Section 5.2 and Figure 5). The observed coverage increases with N : for $N = 400$, the coverage is very close to 95%. We also explored the influence of ϕ_a on the confidence band and coverage probability (not shown here). The higher values of ϕ_a led to the confidence band shrinkage and this in turn resulted in under-coverage of both $\gamma_0(\cdot)$ and $\gamma_1(\cdot)$.

5.4 Estimation in the presence of incomplete information

Since the LongPEER estimate uses external information in the estimation process, it is of interest to evaluate its estimation performance when only partial information is available. In this section, we use a simulation scenario similar to that in Section 5.3, but now the penalty is defined without regard for information about the peak at $s = 0.5$. As displayed in Figure 7, the LongPEER estimates of $\gamma_0(s)$ has appropriate structure at $s = 0.5$, on average. Indeed as with an ordinary ridge penalty, this structure is inherited from the empirical eigenvectors of $W(\cdot)$. This highlights the advantage of an estimate obtained from the jointly-determined eigenvectors of $W(\cdot)$ and L (see Appendix 7); the estimate depends on the relative contributions W and L , controlled by the ratio of ϕ_a to ϕ_b .

The relative increase in the contribution of external information in the estimation process resulted in shrinkage towards zero at $s = 0.5$. The estimates displayed in Figure 7 result from $\phi_b = \phi_a = 1$ (i.e., a ridge penalty) in the middle panel, and $\phi_b = 1$, $\phi_a = 10^{0.75}$ in the bottom panel. For values of ϕ_a larger than $10^{0.75}$, minimal changes in the estimates are observed.

5.5 MRS study application

We applied LongPEER to investigate potential associations of metabolite spectra, obtained from basal ganglia, and the global deficit score (GDS) in a lon-

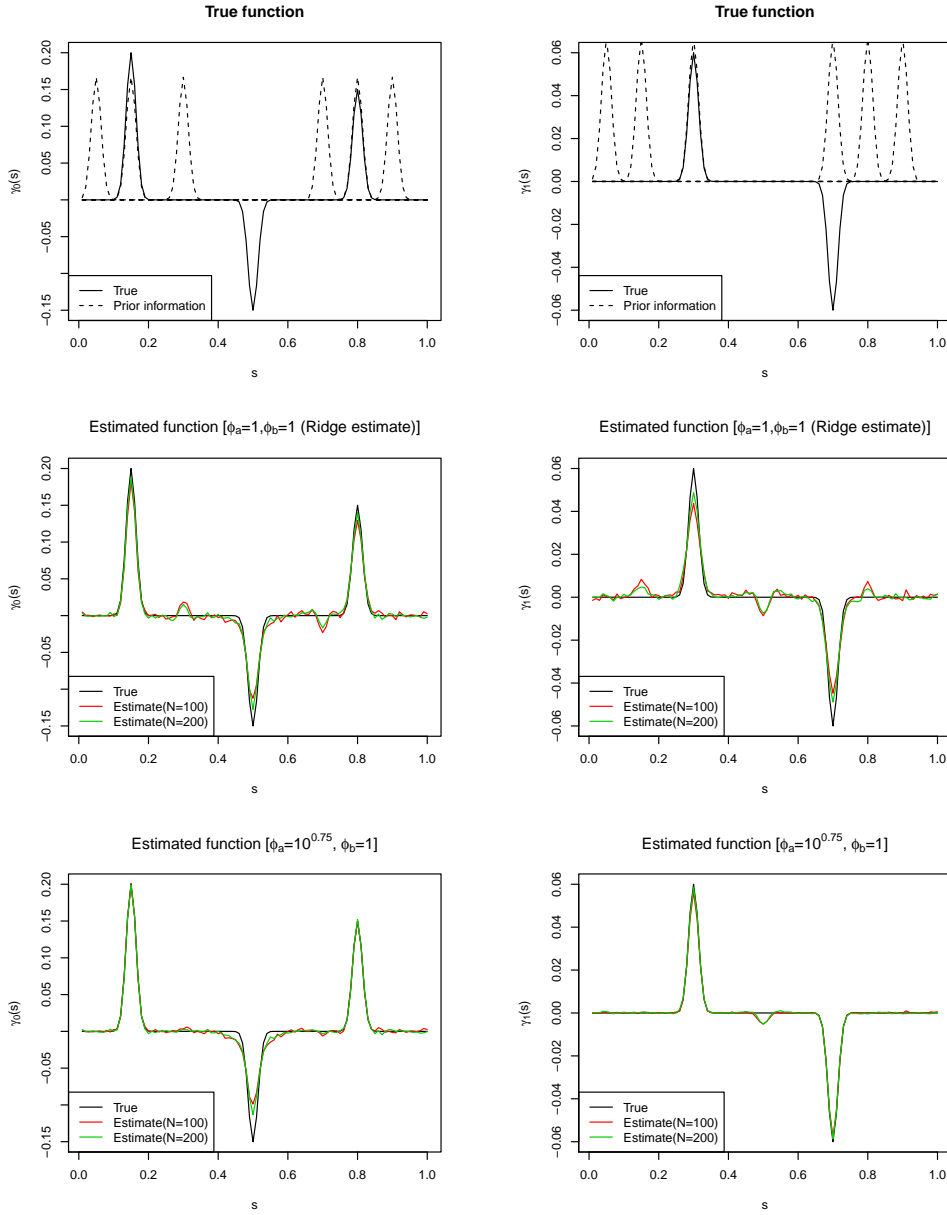


Figure 7: *Top panel:* true regression functions (solid lines) $\gamma_0(\cdot)$ (left) and $\gamma_1(\cdot)$ (right) and 6 vectors spanning P_Q (dashed lines). *Middle panel:* Average ridge-penalty estimate from 100 simulations. *Bottom panel:* Average LongPEER estimate from 100 simulations with P_Q defined by the 6 vectors displayed in the top panel and $\phi_a = 10^{0.75}$.

Table 3: Comparison of AIC for selection of scalar covariates, ϕ_a ($\phi_b = 1$) and time structure in $\gamma(t, \cdot)$ in Section 5.5

	Scalar covariates	Time structure in $\gamma(t, \cdot)$	ϕ_a	AIC
Model 1	t	$\gamma_0(t, \cdot) + t\gamma_1(t, \cdot)$	10	-395.2335
Model 2	Age, t	$\gamma_0(t, \cdot) + t\gamma_1(t, \cdot)$	10	-405.2796
Model 3	Gender, t	$\gamma_0(t, \cdot) + t\gamma_1(t, \cdot)$	10	-395.9040
Model 4	Race, t	$\gamma_0(t, \cdot) + t\gamma_1(t, \cdot)$	10	-398.5607
Model 5	t, t^2	$\gamma_0(t, \cdot) + t\gamma_1(t, \cdot) + t^2\gamma_2(t, \cdot)$	10	-394.5752
Model 6	t	$\gamma_0(t, \cdot) + t\gamma_1(t, \cdot)$	100	-395.3670

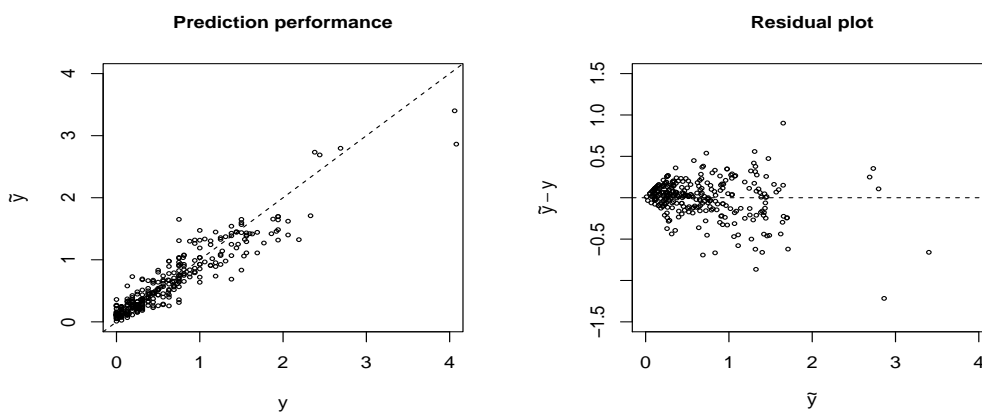


Figure 8: Prediction performance of Model in equation (11). Left panel: observed GDS score (y) and predicted value (\tilde{y}). Right panel: observed \tilde{y} and residuals ($y - \tilde{y}$).

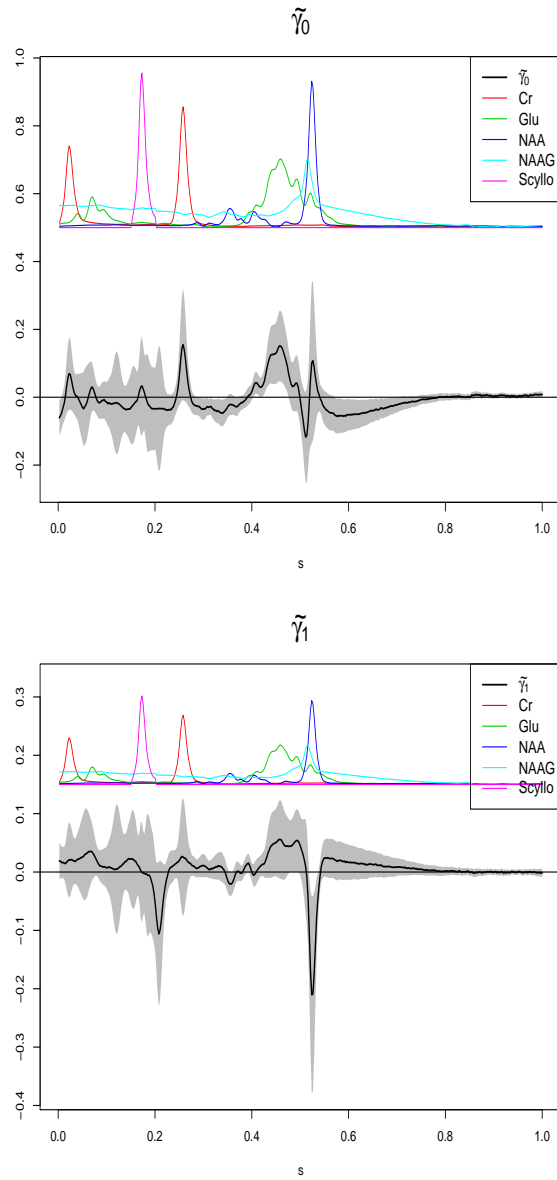


Figure 9: Estimates of the regression function (with 95 % pointwise confidence band) as described in Section 5.5. Shaded region in both the plots represent pointwise confidence bands. Top panel: estimate of $\gamma_0(\cdot)$. Bottom panel: estimate of $\gamma_1(\cdot)$. Selected (scaled) pure metabolite spectra are also shown on both plots. Estimation used a decomposition penalty with $\phi_a = 100$, $\phi_b = 1$.

gitudinal study of late stage HIV patients. Of particular interest is how such an association evolves over time. The study description is available elsewhere (Harezlak et al., 2011). We treat global deficit score (GDS) as our scalar continuous response variable and MR spectrum (sampled at $K = 399$ distinct frequencies) as functional predictor. GDS is often used as a continuous measure of neurocognitive impairment (e.g., Carey et al., 2004) and a large GDS score indicates a high degree of impairment. The MRS spectra are comprised of pure metabolite spectra, instrument noise and a background profile. We collected a total of $n_{\bullet} = 306$ observations from $N = 114$ subjects. The longitudinal observations for each subject were within 3 years from baseline. The number of observations per subject ranged from 1 to 5 with a median equal to 3. Spectral information of 9 pure metabolites was used as prior information for the LongPEER estimation. The pure metabolite spectra are: Creatine (Cr), Glutamate (Glu), Glucose (Glc), Glycerophosphocholine (GPC), *myo*-Inositol (Ins), N-Acetylaspartate (NAA), N-Acetylaspartylglutamate (NAAG), *scyllo*-Inositol (Scyllo) and Taurine (Tau). These spectra are displayed in Figure 1. The decomposition penalty, L_Q , defined as in equation (7) where $Q = [q_1, \dots, q_9]$, is a matrix of dimension 9×399 .

Information available on demographic factors includes: *age* at baseline, *gender* and *race*. We relied on AIC to choose (a) scalar covariates in the model, (b) ϕ_a (while setting $\phi_b = 1$) for defining decomposition based penalty L_Q and (c) the time structure of $\gamma(t, \cdot)$. Based on the AIC (see Table 3), Models 1, 3, 5 and 6 are almost identical and appear to be better than the remaining models. In these models, ϕ_a was selected to be either 10 or 100 and gender is the only scalar covariate. Models 1 and 5 were different with respect to time structure in $\gamma(t, s)$. Although including $\gamma_2(t, \cdot)$ led to a marginal increase in AIC (-394.58 vs -395.23), we did not observe any significantly non-zero region of $\gamma_2(t, \cdot)$, based on pointwise 95% confidence intervals in Model 5. Models 1 and 6 were different in terms of the ϕ_a . Use of smaller ϕ_a led to slight increase in AIC (-395.23 vs -395.37). However, the interpretability of the estimates for $\gamma_0(\cdot)$ and $\gamma_1(\cdot)$ became harder because of their increased wiggleness leading to the choice of Model 6.

Hence, we fit Model 1 (with $\phi_a = 100, \phi_b = 1$) as follows:

$$y_{it} = \beta_0 + \beta_1 t + \int_{\Omega} W_{it}(s)\gamma(t, s)ds + b_i + \epsilon_{it}, \quad (11)$$

where $\gamma(t, s) = \gamma_0(s) + t \gamma_1(s)$ and y_{it} and $W_{it}(\cdot)$ are the GDS and the basal ganglia spectrum for subject i at time t , respectively. We assume that $\epsilon_{it} \sim N(0, \sigma_{\epsilon}^2)$ and b_i is the subject-specific random intercept distributed as $N(0, \sigma_b^2)$. The estimates were obtained as the BLUP from the mixed model formulation described in Section 4.1 using $L_0 = L_1 = L_Q$.

The estimates of λ (tuning parameter) associated with $\gamma_0(\cdot)$ and $\gamma_1(\cdot)$ were 1.152 and 2.242, respectively and the estimates of σ_{ϵ}^2 and σ_b^2 were 0.0786 and 0.3332, respectively. The GDS score, fitted values and residual plot are displayed in Figure 8 for the purpose of model checking. The residuals do not show an obvious pattern indicating lack-of-fit of the proposed model.

Figure 9 displays the estimates of $\gamma_0(\cdot)$ and $\gamma_1(\cdot)$ with pointwise 95% confidence bands. To aid interpretation, selected pure metabolite spectra are displayed. These figures reveal that $\hat{\gamma}_0(\cdot)$ (the ‘‘baseline’’ part of the regression function) is different from zero at the locations where at least one of the pure metabolites Cr, Glu, NAA, NAAG and Scyllo has a bump. Similarly, each non-zero part of $\hat{\gamma}_1(\cdot)$ (the ‘‘longitudinal’’ part of the regression function) coincides with bump locations of one or more pure metabolite profiles of Cr, Glu, NAA, GPC and Ins.

Pointwise confidence intervals for $\gamma_0(\cdot)$ and $\gamma_1(\cdot)$ contain the 0 line over large intervals. The estimated γ_0 is significant in the region $s \in (0.4, 0.5) \cup (0.6, 0.8)$ and estimated γ_1 is significant in a region $s \in (0.5, 0.6)$. To be precise, peaks in both $\hat{\gamma}_0(\cdot)$ and $\hat{\gamma}_1(\cdot)$ are significant at locations where at least one of the pure metabolite profiles NAA or Glu have bumps. The observation of negative ‘longitudinal’ effect of NAA is worth commenting; it suggests that GDS increases as NAA concentration decreases in basal ganglia, a finding consistent with several studies in which a reduced concentration of NAA is seen to be associated with a decrease in neuronal mass (Christiansen et al., 1993; Lim and Spielman, 1997; Soares and Law, 2009).

Finally, we considered other forms of $f(t)$, such as $\exp(t) - 1$ or $\log(t + 1)$. When $\gamma(t, \cdot) = \gamma_0(t, \cdot) + [\exp(t) - 1]\gamma_1(t, \cdot)$ was compared with $\gamma(t, \cdot) = \gamma_0(t, \cdot) +$

$t\gamma_1(t, \cdot)$, the AIC increased to -394.56 from -395.23 . However, the estimation with $\gamma(t, \cdot) = \gamma_0(t, \cdot) + \log(t + 1)\gamma_1(t, \cdot)$ did not show any non-zero regions for $\gamma_1(\cdot)$, using a 95% confidence band. This suggests that other time structures in $\gamma(t, \cdot)$ may be useful, provided longitudinal observations are available for longer time periods.

6 Discussion

We have proposed a novel estimation method for longitudinal functional regression and derived some properties of the estimated coefficient function. A valuable contribution of this framework is that it allows this estimate to vary with time as it extends the scope of penalized regression to the realm of longitudinal data. The approach may be viewed as an extension of longitudinal mixed effects models, replacing scalar predictors by functional predictors. Advantages of this framework include: estimating a time-dependent regression function; the ability to incorporate structural information into the estimation process; easy implementation through the linear mixed model equivalence.

The first simulation study of Section 5.1 illustrates the potential advantage in exploiting an informed structured penalty, as compared to the more generic smoothness or spline-based constraints. The simulation in Section 5.3 suggests that coverage probabilities of the confidence bands for the true regression function are close to the nominal level. However, for small sample sizes the naive confidence bands do not seem to be sufficient and an alternative solution which takes into account the estimation bias is needed. In the case when only partial information is available the proposed method can be still useful, if we limit the relative contribution of the “informed” space and/or increase the sample size (see Subsection 5.4). In the absence of prior information, one may impose more vaguely-defined constraints—such as identity penalties, smoothing penalties or re-weighted projections onto empirical subspaces—to estimate the coefficient function.

Estimation in generalized ridge regression can be expressed in many forms. Clearly, one natural way to view this is via a Bayesian equivalence formulation (see e.g., Robinson, 1991) with the informative priors quantifying the available

scientific knowledge. In our formulation, the linear mixed model equivalence provides an easy computational implementation as well as an automatic choice of the tuning parameters using REML criterion. The GSVD provides algebraic insight and a convenient way to derive the bias and variance expressions of the estimates.

A possible extension of this work is to incorporate multiple functional predictors. For example, given two observed functional predictors $W_t^{(1)}(\cdot)$ and $W_t^{(2)}(\cdot)$, consider two associated coefficient functions: $\gamma^{(1)}(t, \cdot)$ and $\gamma^{(2)}(t, \cdot)$. We can express $\gamma^{(1)}(t, s) = \gamma_0^{(1)}(s) + f_1^{(1)}(t)\gamma_1^{(1)}(s) + \cdots + f_d^{(1)}(t)\gamma_d^{(1)}(s)$ and $\gamma^{(2)}(t, s) = \gamma_0^{(2)}(s) + f_1^{(2)}(t)\gamma_1^{(2)}(s) + \cdots + f_d^{(2)}(t)\gamma_d^{(2)}(s)$. Let $W^{(1)}$ and $W^{(2)}$ represent design matrices for the two functional predictors. Then we can estimate $\gamma^{(1)}(t, \cdot)$ and $\gamma^{(2)}(t, \cdot)$ by finding the BLUP estimate of $\gamma^{(1)}$ and $\gamma^{(2)}$ from the mixed model: $y = X\beta + W^{(1)}\gamma^{(1)} + W^{(2)}\gamma^{(2)} + Zb + \epsilon$. The simplified formula for bias and variance derived in Section 7 still holds with an additional assumption that $(W^{(1)})^\top V^{-1}W^{(2)} = 0$.

As presented here, the method addresses models having a continuous scalar outcome, but allowing for either binary or count responses is of interest. Indeed, an important problem that arises in MRS data is that of understanding the neurocognitive impairment status of HIV patients, defined as a binary variable, based on functional predictors collected over time. Estimation in these general settings appears to be possible with the proposed framework.

Acknowledgment: The authors thank Dr. B. Navia who provided the MRS data used as an example in the manuscript. Partial research support was provided by the National Institutes of Health grants U01-MH083545 (JH), R01-CA126205 (TR) and U01-CA086368 (TR).

7 Connection with the GSVD

We provide the derivation of a LongPEER estimate using the GSVD. This can be viewed as an extension of the estimation discussed by Randolph *et al.* (2012) in two ways: we allow for a general covariance matrix V (for y) and we extend the penalty operator to apply across multiply-defined domains, L_0, \dots, L_D .

After some algebra, the generalized ridge estimate in (6) for γ can be ex-

pressed as

$$\hat{\gamma} = -A_1 X^\top V^{-1} y + A_2 W^\top V^{-1} y$$

where

$$\begin{aligned} A_1^\top &= (X^\top V^{-1} X)^{-1} X^\top V^{-1} W [W^\top V^{-1} W + L^\top L - W^\top V^{-1} X (X^\top V^{-1} X)^{-1} X^\top V^{-1} W]^{-1} \\ A_2 &= W^\top V^{-1} W + L^\top L - W^\top V^{-1} X (X^\top V^{-1} X)^{-1} X^\top V^{-1} W \end{aligned}$$

When $X = 0$ (a situation without any scalar predictors) or $X^\top V^{-1} W = 0$ the generalized ridge estimation of γ can be put into a PEER estimation framework in terms of GS vectors, as discussed below.

With $X = 0$ or $X^\top V^{-1} W = 0$, the $\hat{\gamma}$ reduces to $[W^\top V^{-1} W + L^\top L]^{-1} W^\top V^{-1} y$. Moreover, in this case generalized ridge estimate of β becomes $[X^\top V^{-1} X]^{-1} X^\top V^{-1} y$. Now, if we transform $\tilde{W} := V^{-1/2} W$ and $\tilde{y} := V^{-1/2} y$, we can rewrite L as

$$L = \lambda_0 \text{blockdiag} \left\{ L_0, \frac{\lambda_1}{\lambda_0} L_1, \dots, \frac{\lambda_D}{\lambda_0} L_D \right\} = \lambda_0 L^s$$

Here, L^s can be interpreted as a scaled L where scaling is done for all the tuning parameters associated with the ‘longitudinal’ part of the regression function with respect to the ‘baseline’ tuning parameter.

Set $\tilde{p} = (D + 1)p$, let m denote the number of rows in L and set $c = \dim[\text{Null}(L)]$. Further, assume that $n_\bullet \leq m \leq \tilde{p} \leq m + n_\bullet$ and the rank of the $(n_\bullet + m) \times \tilde{p}$ matrix $[\tilde{W}^\top \quad (L^s)^\top]^\top$ is \tilde{p} . The following describes the GSVD of the pair (\tilde{W}, L^s) : there exist orthogonal matrices \mathcal{U} and \mathcal{V} , a nonsingular \mathcal{G} and diagonal matrices S and M such that

$$\begin{aligned} \tilde{W} &= \mathcal{U} \mathcal{S} \mathcal{G}^{-1} & \mathcal{S} &= [0 \ S] & S &= \text{blockdiag}\{S_1, I_{\tilde{p}-m}\} \\ L^s &= \mathcal{V} \mathcal{M} \mathcal{G}^{-1} & \mathcal{M} &= [M \ 0] & M &= \text{blockdiag}\{I_{\tilde{p}-n_\bullet}, M_1\} \end{aligned}$$

Submatrices S_1 and M_1 have $\ell = n_\bullet + m - \tilde{p}$ diagonal entries ordered as

$$\begin{aligned} 0 < \sigma_1 \leq \sigma_2 \leq \dots \leq \sigma_\ell < 1 & \quad \text{where,} & \quad \sigma_k^2 + \mu_k^2 = 1, & \quad k = 1, \dots, \ell \\ 0 > \mu_1 \geq \mu_2 \geq \dots \geq \mu_\ell > 1 & & & \end{aligned}$$

Here, the columns $\{g_k\}$ of \mathcal{G} are the GS vectors determined by the GSVD of the pair (\tilde{W}, L^s) . Denote the columns of \mathcal{U} and \mathcal{V} by u_k and v_k , respectively. Now, it can be shown that $[W^\top V^{-1} W + L^\top L]^{-1} W^\top V^{-1} = [W^\top V^{-1} W +$

$\lambda_0^2(L^s)^\top L^s]^{-1}W^\top V^{-1} = \mathcal{G}(\mathcal{S}^\top \mathcal{S} + \lambda_0^2 \mathcal{M}^\top \mathcal{M})^{-1} \mathcal{G}^\top \tilde{W}^\top V^{-1/2}$ and consequently, $\hat{\gamma}$ can be expressed as

$$\hat{\gamma} = \mathcal{G}(\mathcal{S}^\top \mathcal{S} + \lambda_0^2 \mathcal{M}^\top \mathcal{M})^{-1} \mathcal{S}^\top \mathcal{U}^\top \tilde{y} = \sum_{k=\tilde{p}-n_\bullet+1}^{\tilde{p}-c} \frac{\sigma_k^2}{\sigma_k^2 + \lambda_0^2 \mu_k^2} \frac{1}{\sigma_k} u_k^\top \tilde{y} g_k + \sum_{k=\tilde{p}-c+1}^{\tilde{p}} u_k^\top \tilde{y} g_k$$

Further, the bias and variance can be expressed as

$$\begin{aligned} \text{Bias}[\hat{\gamma}] &= (I - W^\# W) \gamma = \mathcal{G}(\mathcal{S}^\top \mathcal{S} + \lambda_0^2 \mathcal{M}^\top \mathcal{M})^{-1} (\lambda_0^2 \mathcal{M}^\top \mathcal{M}) \mathcal{G}^{-1} \\ &= \sum_{k=1}^{\tilde{p}-n_\bullet} g_k \tilde{g}_k^\top \gamma + \sum_{k=\tilde{p}-n_\bullet+1}^{\tilde{p}-c} \frac{\lambda_0^2 \mu_k^2}{\sigma_k^2 + \lambda_0^2 \mu_k^2} g_k \tilde{g}_k^\top \gamma \end{aligned}$$

$$\begin{aligned} \text{Var}[\hat{\gamma}] &= W^\# V (W^\#)^\top = \mathcal{G}(\mathcal{S}^\top \mathcal{S} + \lambda_0^2 \mathcal{M}^\top \mathcal{M})^{-1} \mathcal{S}^\top \mathcal{S} (\mathcal{S}^\top \mathcal{S} + \lambda_0^2 \mathcal{M}^\top \mathcal{M})^{-1} \mathcal{G}^\top \\ &= \sum_{k=\tilde{p}-n_\bullet+1}^{\tilde{p}-c} \frac{\sigma_k^2}{(\sigma_k^2 + \lambda_0^2 \mu_k^2)^2} g_k g_k^\top + \sum_{k=\tilde{p}-c+1}^{\tilde{p}} g_k g_k^\top \end{aligned}$$

where, $W^\# = [W^\top V^{-1} W + L^\top L]^{-1} W^\top V^{-1}$ and \tilde{g}_k denotes the k th column of $\mathcal{G}^{-T} = (\mathcal{G}^{-1})^\top = (\mathcal{G}^\top)^{-1}$. Further, we can express bias as $[W^\top V^{-1} W + L^\top L]^{-1} L^\top L \gamma$ which means $\hat{\gamma}$ will be unbiased only when $\gamma \in \text{Null}(L)$.

For estimates obtained using this technique, the bias and variance can be expressed in terms of generalized singular vectors, provided the assumption of $X^\top V^{-1} W = 0$ applies. In this case, one can show that $\hat{\beta}$ is simply the generalized least squares estimate from the linear model $y = X\beta + \epsilon^*$, and $\hat{\gamma}$ is the generalized ridge estimate from $y = W\gamma + \epsilon^*$ with penalty L . That is, β is estimated as if $W\gamma$ were not present, and γ is estimated as if $X\beta$ were not present.

Bibliography

- Bjorck, A. (1996). Numerical methods for least square problems, 1st edition. Philadelphia: SIAM.
- Brumback, B. and Rice J. (1998). Smoothing spline models for the analysis of nested and crossed samples of curves. *Journal of American Statistical Association* **93(443)**, 961–976.
- Cai, T. and Hall, P. (2006). Prediction in functional linear regression. *The Annals of Statistics* **34(5)**, 2159–2179.
- Cardot, H., Ferraty, F. and Sarda, P. (1999). Functional linear model. *Statistics and Probability Letters* **45(1)**, 11–22.
- Cardot, H., Ferraty, F. and Sarda, P. (2003). Spline estimators for the functional linear model. *Statistica Sinica* **13**, 571–591.
- Cardot, H., Crambes, C., Kneip, A. and Sarda, P. (2007). Smoothing splines estimators in functional linear regression with errors-in-variables. *Computational Statistics Data Analysis* **51(10)**, 4832–4848.
- Carey, C., Woods, S., Gonzalez, R., Conover, E., Marcotte, T., Grant, I. and Heaton, R. (2004). Predictive validity of global deficit scores in detecting neuropsychological impairment in HIV infection. *Journal of Clinical and Experimental Neuropsychology* **26(3)**, 307–319.
- Christiansen, P., Toft, P., Larsson, H., Stubgaard, M. and Henriksen, O. (1993). The concentration of N-acetyl aspartate, creatine + phosphocreatine, and choline in different parts of the brain in adulthood and senium. *Magnetic resonance imaging* **11(6)**, 799–806.

- Crainiceanu, C., Reiss, P., Goldsmith, A., Huang, L., Huo, L. and Scheipl F. (2012). `refund`: Regression with Functional Data (R package version 0.1-6). [<http://CRAN.R-project.org/package=refund>].
- Di, C., Crainiceanu, C., Caffo, B. and Punjabi, N. (2009). Multilevel functional principal component analysis. *Annals of Applied Statistics* **4**, 458–288.
- Engl, H. W., Hanke, M. and Neubauer, A. (2000). Regularization of Inverse Problems, Kluwer Academic Publishers.
- Fan J., and Zhang, J. (2000). Two-step estimation of functional linear models with applications to longitudinal data. *Journal of the Royal Statistical Society: Series B (Statistical Methodology)* **62(2)**, 303–322.
- Faraway, J. (1997). Regression analysis for a functional response. *Technometrics* **39(3)**, 254–261.
- Fitzmaurice, M., Laird, G. and Ware, J. (2004). Applied Longitudinal Analysis, 1st edition. Wiley Series in probability and statistics.
- Gertheiss, J., Goldsmith, J., Crainiceanu, C., and Greven, S. (2013). Longitudinal scalar-on-functions regression with application to tractography data. *Biostatistics* **14(3)**, 447–461.
- Goldsmith, J., Bobb, J., Crainiceanu, C., Caffo, B. and Reich, D. (2011). Penalized functional regression. *Journal of Computational and Graphical Statistics* **20(4)**, 830–851.
- Goldsmith, J., Bobb, J., Crainiceanu, C., Caffo, B. and Reich, D. (2012). Longitudinal penalized functional regression for cognitive outcomes on neuronal tract measurements. *Journal of the Royal Statistical Society: Series C (Applied Statistics)* **61(3)**, 453–469.
- Golub G. and Van-Loan C. (1996) Matrix computations, Baltimore: John Hopkins University Press.
- Greven, S., Crainiceanu, C., Caffo, B. and Reich, D. (2011). Longitudinal functional principal component analysis. Recent Advances in Functional Data Analysis and Related Topics, 1st Edition. Physica-Verlag HD pp.149–154.

- Guo, W. (2002). Functional mixed effects models. *Biometrics* **58(1)**, 121–128.
- Hall, P., Poskitt, D., and Presnell, B. (2001). A functional data-analytic approach to signal discrimination. *Technometrics* **43(1)**, 1–9.
- Harezlak, J., Buchthal, S., Taylor, M., Schifitto, G., Zhong, J., Daar, E., Alger, J., Singer, E., Campbell, T. and Yiannoutsos, C. (2011). Persistence of HIV-associated cognitive impairment, inflammation, and neuronal injury in era of highly active antiretroviral treatment. *AIDS* **25**, 625–633.
- Henderson, C. (1950). Estimation of genetic parameters (abstract). *Annals of Mathematical Statistics* **21(1)**.
- Hoerl, A.E. and Kennard, R.W. (1970). Ridge Regression: Biased Estimation for Nonorthogonal Problems. *Technometrics* **12(1)**, 55–67.
- James, G. (2002). Generalized linear models with functional predictors. *Journal of the Royal Statistical Society: Series B (Statistical Methodology)* **64(3)**, 411–432.
- Lim, K. and Spielman, D. (1997). Estimating NAA in cortical gray matter with applications for measuring changes due to aging. *Magnetic resonance in medicine* **37(3)**, 372–377.
- Morris, J. and Carroll, R. (2006). Wavelet-based functional mixed models. *Journal of the Royal Statistical Society: Series B (Statistical Methodology)* **68(2)** 179–199.
- Müller, H. (2005). Functional modelling and classification of longitudinal data. *Scandinavian Journal of Statistics* **32(2)**, 223–240.
- Müller, H. and Stadtmüller, U. (2005). Generalized functional linear models. *The Annals of Statistics* **33(2)**, 774–805.
- Paige, C. and Saunders, M. (1981). Towards a generalized singular value decomposition. *SIAM Journal on Numerical Analysis* **18(3)**, 398–405.
- Phillips, D. L. (1962), A technique for the numerical solution of certain integral equations of the first kind, *J. Associat. Comput. Mach.*, **9**, 84–97.

- Ramsay, J. and Dalzell, C. (1991). Some tools for functional data analysis. *Journal of the Royal Statistical Society. Series B (Methodological)* **53(3)**, 539–572.
- Ramsay, J. and Silverman, B. (1997). *Functional Data Analysis*, 1st edition. Springer-Verlag, Berlin.
- Randolph, T., Harezlak, J. and Feng, Z. (2012). Structured penalties for functional linear models – partially empirical eigenvectors for regression. *Electronic Journal of Statistics* **6**, 323–353.
- Reiss, P. and Ogden, R. (2009). Smoothing parameter selection for a class of semiparametric linear models. *Journal of the Royal Statistical Society: Series B (Statistical Methodology)* **71(2)**, 505–523.
- Robinson, G. (1991). That blup is a good thing: the estimation of random effects. *Statistical Science* **6(1)**, 15–32.
- Ruppert, D., Wand, M. and Carroll, R. (2003). *Semiparametric Regression*, 1st edition. Cambridge Series in Statistical and Probabilistic Mathematics.
- Salganik, M. and Wand, M. and Lange, N. (2004). Comparison of Feature Significance Quantile Approximations. *Australian & New Zealand Journal of Statistics* **46(4)**, 569–581.
- Silverman, B.W. (1996). Smoothed functional principal components analysis by choice of norm. *Annals of Statistics* **24**, 1–24.
- Soares, D. and Law, M. (2009). Magnetic resonance spectroscopy of the brain: review of metabolites and clinical applications. *Clinical radiology* **64(1)**, 12–21.
- Tikhonov, A. N. (1963), Solution of incorrectly formulated problems and the regularization method, *Dokl. Akad. Nauk SSSR*, **151(3)**, 501–504 (in Russian); *English transl.: Soviet Math. Dokl.*, **4(4)**, 1035–1038.
- Van-Loan, C. (1976). Generalizing the singular value decomposition. *SIAM Journal on Numerical Analysis* **13(1)**, 76–83.
- Yao, F. and Müller, H. (2010). Functional quadratic regression. *Biometrika* **97(1)**, 49–64.

Department of Biostatistics

Indiana University Fairbanks School of Public Health

E-mail: mgkundu@iupui.edu

E-mail: harezlak@iupui.edu